

Canonical interpretation of $Y(10750)$ and $\Upsilon(10860)$ in the Υ family

Qi Li, Ming-Sheng Liu, Qi-Fang Lü^{*}, Long-Cheng Gui[†], and Xian-Hui Zhong[‡]

1) Department of Physics, Hunan Normal University, Changsha 410081, China

2) Synergetic Innovation Center for Quantum Effects and Applications (SICQEA), Changsha 410081, China and

3) Key Laboratory of Low-Dimensional Quantum Structures and Quantum Control of Ministry of Education, Changsha 410081, China

Inspired by the new resonance $Y(10750)$, we calculate the masses and two-body OZI-allowed strong decays of the higher vector bottomonium states within both screened and linear potential models. We discuss the possibilities of $\Upsilon(10860)$ and $Y(10750)$ as mixed states via the $S - D$ mixing. Our results suggest that $Y(10750)$ and $\Upsilon(10860)$ might be explained as mixed states between $5S$ - and $4D$ -wave vector $b\bar{b}$ states. The $Y(10750)$ and $\Upsilon(10860)$ resonances may correspond to the mixed states dominated by the $4D$ - and $5S$ -wave components, respectively. The mass and the strong decay behaviors of the $\Upsilon(11020)$ resonance are consistent with the assignment of the $\Upsilon(6S)$ state in the potential models.

PACS numbers:

I. INTRODUCTION

Very recently, the Belle Collaboration reported a new measurement of the $e^+e^- \rightarrow \Upsilon(nS)\pi^+\pi^-$ ($n = 1, 2, 3$) cross sections at energies from 10.52 to 11.02 GeV using data collected with the Belle detector at the KEKB asymmetric-energy e^+e^- collider [1]. Besides two old vector states $\Upsilon(10860)$ and $\Upsilon(11020)$, a new resonance near 10.75 GeV, i.e. $Y(10750)$ as named in Ref. [2], was obviously found in the cross sections. The Breit-Wigner mass and width of this new structure are found to be $M = (10752.7 \pm 5.9^{+0.7}_{-1.1})$ MeV and $\Gamma = (35.5^{+17.6+3.9}_{-11.3-3.3})$ MeV. The production processes indicate that the spin-parity numbers of these three states appearing in the cross sections should be $J^{PC} = 1^{--}$. It is a great challenge for our understanding these states with the conventional S -, and D -wave bottomonium ($b\bar{b}$) states in the potential models.

The general consensus is that $\Upsilon(10860)$ and $\Upsilon(11020)$ correspond to the S -wave vector $b\bar{b}$ states $\Upsilon(5S)$ and $\Upsilon(6S)$, respectively [3–12]. However, if one assigns $\Upsilon(10860)$ to $\Upsilon(5S)$, we should face several problems, such as (i) the mass of $\Upsilon(5S)$ from the recent potential model calculations is about 70 – 90 MeV lower than the observed value of $\Upsilon(10860)$ [8–12]; (ii) the mass splittings $m[\Upsilon(5S) - \Upsilon(4S)]_{\text{th}} \approx 210$ MeV and $m[\Upsilon(6S) - \Upsilon(5S)]_{\text{th}} \approx 180$ MeV predicted within various potential models [8–12] are inconsistent with the observations $m[\Upsilon(5S) - \Upsilon(4S)]_{\text{exp}} \approx 306$ MeV and $m[\Upsilon(6S) - \Upsilon(5S)]_{\text{exp}} \approx 115$ MeV.

For the newly observed $Y(10750)$, we also meet several problems if we explain it with a pure S -, or D -wave vector bottomonium state. According to the predictions in potential models, the $Y(10750)$ resonance lies between the vector states $\Upsilon(5S)$ and $\Upsilon_1(3D)$ [7–11]. Thus, if the $Y(10750)$ resonance correspond to a pure vector $b\bar{b}$ state, it should be assigned to either $\Upsilon(5S)$ or $\Upsilon_1(3D)$. However, if one assigns the $Y(10750)$ resonance to $\Upsilon(5S)$, we should meet a problem at once: how do we assign the $\Upsilon(10860)$ in the bottomonium

family? On the other hand, if one assigns the $Y(10750)$ resonance to the $\Upsilon_1(3D)$ state, we cannot understand the productions of $Y(10750)$ in the $e^+e^- \rightarrow \Upsilon(nS)\pi^+\pi^-$ ($n = 1, 2, 3$) processes, where the production cross sections of the D -wave states should be strongly suppressed for their very tiny dielectron widths predicted in theory [8, 11, 13, 14].

The above analysis indicates that both $\Upsilon(10860)$ and $Y(10750)$ cannot be simply explained with a pure S - or D -wave $b\bar{b}$ state with $J^{PC} = 1^{--}$. Thus, in the literature these resonances were suggested to be exotic states, such as, compact tetraquarks [2, 15], or hadrobottomonium [16]. It should be emphasized that although $\Upsilon(10860)$ and $Y(10750)$ are not good candidates of a pure S - or D -wave $b\bar{b}$ states, we cannot exclude them as mixed states between the S - and D -wave vector $b\bar{b}$ states. In Refs. [13, 14], Badalian *et al.* studied the dielectron widths of the vector bottomonium states, their results indicate that there might be sizeable $S - D$ mixing between the nS - and $(n - 1)D$ -wave ($n \geq 4$) vector states. If there is $S - D$ mixing indeed, the masses of the pure S - and D -wave states should be shifted to the physical states by some interactions. Then we may overcome the mass puzzles of the $\Upsilon(10860)$ as a pure $\Upsilon(5S)$ state. On the other hand, if there is $S - D$ mixing indeed, the physical states might have sizeable components of both S - and D -wave states. Considering the $Y(10750)$ as a mixed state dominated by the D -wave component, we may explain the large production cross sections in the $e^+e^- \rightarrow \Upsilon(nS)\pi^+\pi^-$ ($n = 1, 2, 3$) processes for its sizeable S -wave component. In fact, the $S - D$ mixing might also exist in the other meson spectra, such as the $\psi(3770)$ is suggested to be a 1^3D_1 state with a small admixture of 2^3S_1 state in the $c\bar{c}$ family [5, 17–19], while the $D_s^*(2600)$ and $D_{s1}^*(2700)$ might be mixed states via the $2^3S_1 - 1^3D_1$ mixing in the D and D_s meson families, respectively [20–26].

In this work, we discuss the possibilities of $\Upsilon(10860)$ and $Y(10750)$ as mixed states via the $S - D$ mixing. By analyzing the mass spectrum of higher vector bottomonium states above the $B\bar{B}$ threshold within both screened and linear potential models, and calculating their strong decays with the 3P_0 model, we suggest that $Y(10750)$ and $\Upsilon(10860)$ might correspond to the two mixed states between $5S$ - and $4D$ -wave vector $b\bar{b}$ states with a sizeable mixing angle. The $Y(10750)$ and $\Upsilon(10860)$ resonances could be the $S - D$ mixed states domi-

^{*}E-mail: lvqifang@hunnu.edu.cn

[†]E-mail: guilongcheng@hunnu.edu.cn

[‡]E-mail: zhongxh@hunnu.edu.cn

nated by the 4D- and 5S-wave components, respectively.

This paper is organized as follows. The mass spectrum of higher vector bottomonium is calculated in Sec. II. The 3P_0 model is briefly introduced and strong decays the vector $b\bar{b}$ states are calculated in Sec. III. Then, combining the mass and widths, we carry out a discussion about the properties of the $J^{PC} = 1^{--}$ states $Y(10750)$, $Y(10860)$ and $Y(11020)$ in Sec. IV. Finally, a short summary is presented in Sec. V.

II. MASS SPECTRUM

The mass spectrum of bottomonium has been calculated in our previous works [10, 27] within the widely used linear potential model [5, 7, 28–31] and screened potential model [3, 32–35]. In these potential models, the effective potential of spin-independent term $V(r)$ is regarded as the sum of Lorentz vector $V_V(r)$ and Lorentz scalar $V_S(r)$ contributions [5], i.e.,

$$V(r) = V_V(r) + V_S(r). \quad (1)$$

The Lorentz vector potential $V_V(r)$ can be written as the standard color Coulomb form

$$V_V(r) = -\frac{4}{3} \frac{\alpha_s}{r}. \quad (2)$$

The Lorentz scalar potential $V_S(r)$ might be taken as a simple form with a linear potential [5, 7, 28, 29, 31] or the screened potential as suggested in Refs. [3, 32–35], i.e.,

$$V_S(r) = \begin{cases} br & \text{Linear potential} \\ \frac{b(1-e^{-\mu r})}{\mu} & \text{Screened potential.} \end{cases} \quad (3)$$

Furthermore, we include three spin-dependent terms as follows. For the spin-spin contact hyperfine potential, we take [31]

$$H_{SS} = \frac{32\pi\alpha_s}{9m_b^2} \tilde{\delta}_\sigma(r) \mathbf{S}_b \cdot \mathbf{S}_{\bar{b}}, \quad (4)$$

where \mathbf{S}_b and $\mathbf{S}_{\bar{b}}$ are spin matrices acting on the spins of the quark and antiquark. We take $\tilde{\delta}_\sigma(r) = (\sigma/\sqrt{\pi})^3 e^{-\sigma^2 r^2}$ as in Ref. [31]. For the spin-orbit and the tensor terms, we adopt [5]:

$$H_{SL} = \frac{1}{2m_b^2 r} \left(3 \frac{dV_V}{dr} - \frac{dV_S}{dr} \right) \mathbf{L} \cdot \mathbf{S}, \quad (5)$$

and

$$H_T = \frac{1}{12m_b^2} \left(\frac{1}{r} \frac{dV_V}{dr} - \frac{d^2 V_V}{dr^2} \right) S_T, \quad (6)$$

where \mathbf{L} is the relative orbital angular momentum of b and \bar{b} quarks, $\mathbf{S} = \mathbf{S}_b + \mathbf{S}_{\bar{b}}$ is the total quark spin, and the spin tensor S_T is defined by [5]

$$S_T = 6 \frac{\mathbf{S} \cdot \mathbf{r} \mathbf{S} \cdot \mathbf{r}}{r^2} - 2\mathbf{S}^2. \quad (7)$$

If the linear potential is adopted, four parameters (α_s , b , m_b , σ) in the above equations should be determined, while if the screened potential is adopted, five parameters (α_s , b , m_b , σ , μ) should be determined.

We solve the radial Schrödinger equation by using the three-point difference central method [36]. With this method, one can reasonably include the corrections from these spin-dependent potentials to both the mass and wave function of a meson state. The details of the numerical method can be found in our previous works [10, 37]. With the same parameter sets determined in our previous works, we calculated the masses of the vector $b\bar{b}$ states, nS ($n = 4, 5, 6$), nD ($n = 3, 4, 5$), above the $B\bar{B}$ threshold within both the linear and screened potential models.

The calculated bottomonium masses are listed in Table I and also shown in Fig. 1. It is found that both the linear and screened potential models give a similar prediction of the masses. Considering the $Y(10580)$ and $Y(11020)$ resonances as the $Y(4S)$ and $Y(6S)$ states, respectively, their observed masses are in good agreement with the potential model predictions. However, considering the $Y(10860)$ as the $Y(5S)$ state, the observed mass is obviously (about 70 – 90 MeV) larger than the model predictions. Fig. 1 shows that the newly observed state $Y(10750)$ lies about 100 MeV above $Y_1(3D)$, while about 40 – 50 MeV below $Y(5S)$.

III. STRONG DECAYS

In this section, we use the 3P_0 model [38–40] to evaluate the Okubo-Zweig-Iizuka (OZI) allowed two-body strong decays of the vector bottomonium. In this model, it assumes that the vacuum produces a light quark-antiquark pair with the quantum number 0^{++} and the bottomonium decay takes place though the rearrangement of the four quarks. The transition operator \hat{T} can be written as

$$\begin{aligned} \hat{T} = & -3\gamma \sqrt{96\pi} \sum_m \langle 1m1 - m | 00 \rangle \int d\mathbf{p}_3 d\mathbf{p}_4 \delta^3(\mathbf{p}_3 + \mathbf{p}_4) \\ & \times \mathcal{Y}_1^m \left(\frac{\mathbf{p}_3 - \mathbf{p}_4}{2} \right) \chi_{1-m}^{34} \phi_0^{34} \omega_0^{34} b_{3i}^\dagger(\mathbf{p}_3) d_{4j}^\dagger(\mathbf{p}_4), \end{aligned} \quad (8)$$

where γ is a dimensionless constant that denotes the strength of the quark-antiquark pair creation with momentum \mathbf{p}_3 and \mathbf{p}_4 from vacuum; $b_{3i}^\dagger(\mathbf{p}_3)$ and $d_{4j}^\dagger(\mathbf{p}_4)$ are the creation operators for the quark and antiquark, respectively; the subscriptions, i and j , are the SU(3)-color indices of the created quark and anti-quark; $\phi_0^{34} = (u\bar{u} + d\bar{d} + s\bar{s})/\sqrt{3}$ and $\omega_0^{34} = \frac{1}{\sqrt{3}}\delta_{ij}$ correspond to flavor and color singlets, respectively; χ_{1-m}^{34} is a spin triplet state; and $\mathcal{Y}_{\ell m}(\mathbf{k}) \equiv |\mathbf{k}|^\ell Y_{\ell m}(\theta_{\mathbf{k}}, \phi_{\mathbf{k}})$ is the ℓ -th solid harmonic polynomial.

For an OZI allowed two-body strong decay process $A \rightarrow B+C$, the helicity amplitude $\mathcal{M}^{M_{J_A} M_{J_B} M_{J_C}}(\mathbf{P})$ can be calculated as follow

$$\langle BC|T|A \rangle = \delta(\mathbf{P}_A - \mathbf{P}_B - \mathbf{P}_C) \mathcal{M}^{M_{J_A} M_{J_B} M_{J_C}}(\mathbf{P}). \quad (9)$$

With the Jacob-Wick formula [41], the helicity amplitudes

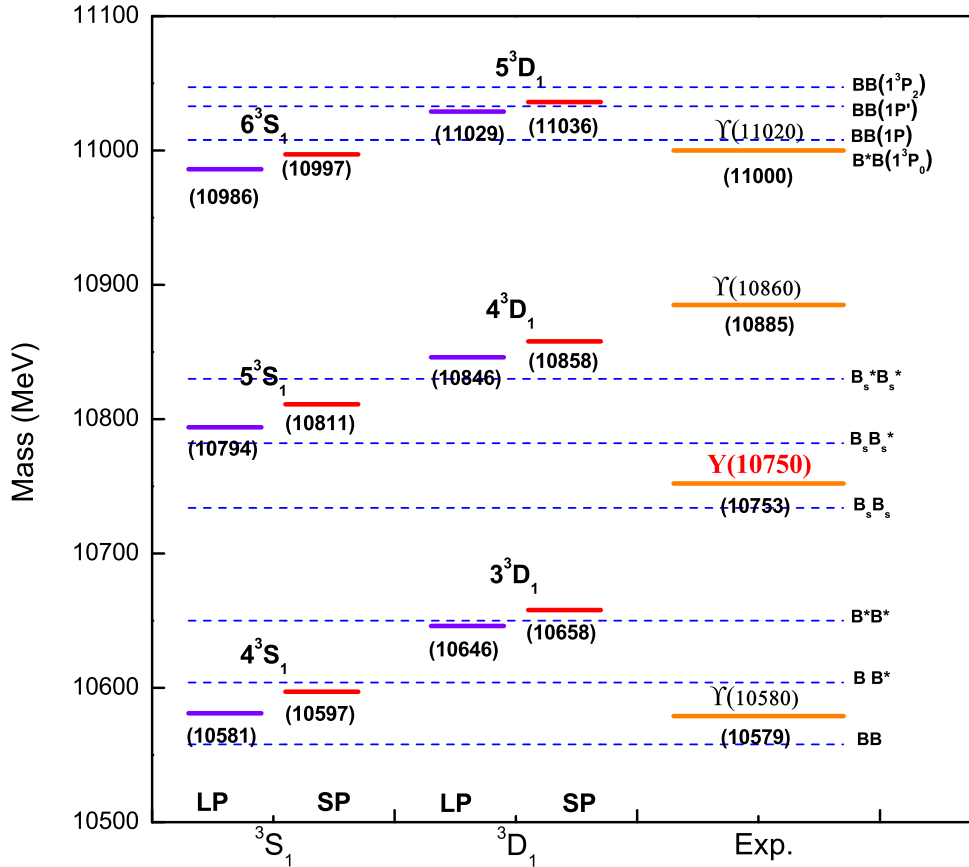


FIG. 1: The spectrum of the higher vector bottomonium above the $B\bar{B}$ threshold predicted within both screened potential (SP) and linear potential (LP) models. For a comparison, the experimental observations [1, 45] are plotted in the figure as well.

TABLE I: Predicted masses (MeV) of higher vector bottomonium states with both the linear potential (LP) and screened potential (SP) models. For a comparison, the results from recent works and experimental observations are also listed.

State	$n^{2S+1}L_J$	LP	SP	Ref. [11]	Ref. [8]	Ref. [9]	Exp.
$\Upsilon(4S)$	4^3S_1	10581	10597	10612	10635	10607	10579 [45]
$\Upsilon(5S)$	5^3S_1	10794	10811	10822	10878	10818	10885 [1]
$\Upsilon(6S)$	6^3S_1	10986	10997	11001	11102	10995	11000 [1]
$\Upsilon_1(3D)$	3^3D_1	10646	10658	10675	10698	10653	...
$\Upsilon_1(4D)$	4^3D_1	10846	10858	10871	10928	10853	...
$\Upsilon_1(5D)$	5^3D_1	11029	11036	11041	...	11023	...

$\mathcal{M}^{M_{J_A} M_{J_B} M_{J_C}}(\mathbf{P})$ can be converted to the partial wave amplitudes \mathcal{M}^{JL} via

$$\mathcal{M}^{JL}(A \rightarrow BC) = \frac{\sqrt{4\pi(2L+1)}}{2J_A+1} \sum_{M_{J_B}, M_{J_C}} \langle L0JM_{J_A} | J_A M_{J_A} \rangle \times \langle J_B M_{J_B} J_C M_{J_C} | J M_{J_A} \rangle \mathcal{M}^{M_{J_A} M_{J_B} M_{J_C}}(\mathbf{P}). \quad (10)$$

In the above equations, $(J_A, J_B$ and $J_C)$, $(L_A, L_B$ and $L_C)$ and

$(S_A, S_B$ and $S_C)$ are the quantum numbers of the total angular momenta, orbital angular momenta and total spin for hadrons A, B, C , respectively; $M_{J_A} = M_{J_B} + M_{J_C}$, $\mathbf{J} \equiv \mathbf{J}_B + \mathbf{J}_C$ and $\mathbf{J}_A \equiv \mathbf{J}_B + \mathbf{J}_C + \mathbf{L}$. In the c.m. frame of hadron A , the momenta \mathbf{P}_B and \mathbf{P}_C of mesons B and C satisfy $\mathbf{P}_B = -\mathbf{P}_C \equiv \mathbf{P}$.

To partly remedy the inadequacy of the nonrelativistic wave function as the momentum \mathbf{P} increases, a Lorentz boost factor

γ_f is introduced into the decay amplitudes [42],

$$\mathcal{M} \rightarrow \gamma_f \mathcal{M}(\gamma_f \mathbf{P}). \quad (11)$$

where $\gamma_f = M_B/E_B$. In the decays with small phase space, the three momenta \mathbf{P} carried by the final state mesons and corrections from the Lorentz boost are relatively small, while the relativistic effects may be essential for the decay channels with larger phase space.

Finally, the partial width $A \rightarrow B + C$ can be given by

$$\Gamma = 2\pi |\mathbf{P}| \frac{E_B E_C}{M_A} \sum_{JL} |\mathcal{M}^{JL}|^2, \quad (12)$$

where M_A is the mass of the initial hadron A , while E_B and E_C stand for the energies of final hadrons B and C , respectively. The details of the formula of the 3P_0 model can be found in Refs [42, 43].

In the calculations, the wave functions of the initial vector bottomonium states are taken from our quark model predictions. Furthermore, we need the wave functions of the final hadrons, i.e., the $B^{(*)}$ and $B_s^{(*)}$ mesons and some of their excitations, which are adopted from the quark model predictions of Refs. [23, 44]. The masses of the final hadron states in the decay processes are adopted from the Particle Data Group [45] if there are data, while if there are no observations we adopt the predicted values from Refs. [23, 44]. The quark pair creation strength is determined to be $\gamma = 0.232$ by reproducing the measured width $\Upsilon(10580) \rightarrow B\bar{B} = 20.5$ MeV [45] with the wave function calculated from the screened potential model. The γ determined in this work is also close to the values 0.217/0.234 adopted in the study of the strong decays of excited charmonium states [42]. The strong decay properties for the vector bottomonium are presented in Table II. It is found that both the linear and screened potential models give similar predictions for the strong decay properties of the bottomonium states.

IV. DISCUSSIONS

A. $Y(10750)$ and $Y(10860)$

For the $Y(10860)$ resonance, the mass and spin-parity numbers indicate that it may be a candidate of the conventional $\Upsilon_1(4D)$. However, with this assignment it is found that the total decay width, ~ 81 MeV (see Table III), is about a factor of 2 larger than the measured width ~ 37 MeV [1]. Furthermore, assigning $Y(10860)$ as $\Upsilon_1(4D)$ we will meet a problem in the explanation of its productions in the $e^+e^- \rightarrow \Upsilon(nS)\pi^+\pi^-$ ($n = 1, 2, 3$), because the production rates of D -wave states should be strongly suppressed for their tiny dielectron widths [8, 9, 11, 13, 14]. The $Y(10860)$ resonance is often explained as the $\Upsilon(5S)$ state in the literature [7–9, 11], with this assignment, the total width is predicted to be ~ 44 MeV (see Table IV), which is consistent with the data. However, if we assign $Y(10860)$ to $\Upsilon(5S)$ we should face some problems, for example, (i) the predicted mass of $\Upsilon(5S)$ state is about 70 MeV lower than that of $Y(10860)$;

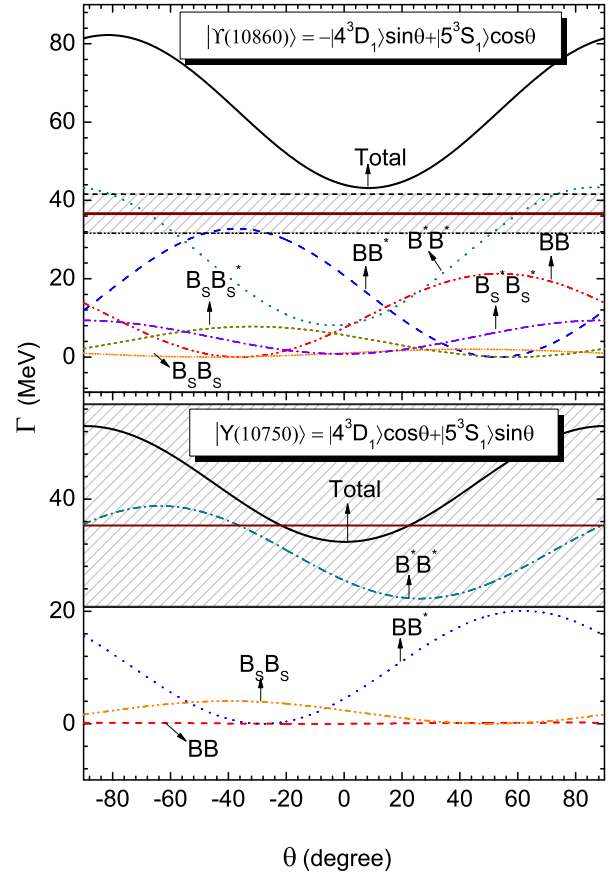


FIG. 2: Strong decays of $Y(10750)$ and $Y(10860)$ versus the mixing angle θ within screened potential model.

(ii) moreover, the mass splittings $m[\Upsilon(5S) - \Upsilon(4S)]_{\text{th}} \simeq 210$ MeV and $m[\Upsilon(6S) - \Upsilon(5S)]_{\text{th}} \simeq 180$ MeV predicted within various potential models (see Table I) are inconsistent with the observations $m[\Upsilon(5S) - \Upsilon(4S)]_{\text{exp}} \simeq 306$ MeV and $m[\Upsilon(6S) - \Upsilon(5S)]_{\text{exp}} \simeq 115$ MeV [45].

For the new structure $Y(10750)$ observed at Belle, from Figure 1 one finds that it lies between the vector states $\Upsilon(5S)$ and $\Upsilon_1(3D)$. The predicted mass of $\Upsilon_1(3D)$ state is about 100 MeV lower than that of $Y(10750)$. If one assigns the $Y(10750)$ resonance to the $\Upsilon_1(3D)$ state, we cannot understand its production rates in the $e^+e^- \rightarrow \Upsilon(nS)\pi^+\pi^-$ ($n = 1, 2, 3$) processes. The production cross sections of the D -wave states should be strongly suppressed for their very tiny dielectron widths predicted in theory [8, 9, 11, 13, 14]. Thus, the explanation of the $Y(10750)$ resonance as the $\Upsilon_1(3D)$ state should be excluded. On the other hand, if one assigns the $Y(10750)$ resonance to $\Upsilon(5S)$, it is found that the decays of $Y(10750)$ are dominated by the B^*B^* channel, and the decay width is predicted to be $\Gamma \sim 53$ MeV, which is close to the measured value $35.5^{+17.6+3.9}_{-11.3-3.3}$ MeV at Belle [1]. However, we will meet a prob-

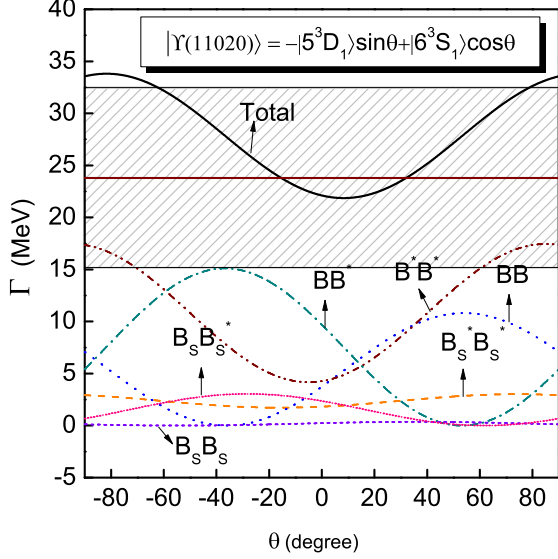


FIG. 3: Strong decay of $\Upsilon(11020)$ versus the mixing angle θ within screened potential model.

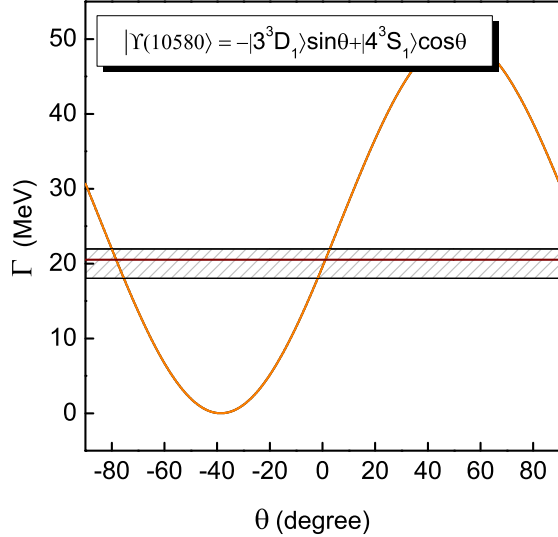


FIG. 4: Strong decay of $\Upsilon(10580)$ versus the mixing angle θ within screened potential model.

lem that there are no S -wave vector states to be assigned to $\Upsilon(10860)$, then we cannot understand largest production rates of $\Upsilon(10860)$ in the $e^+e^- \rightarrow \Upsilon(nS)\pi^+\pi^-$ ($n = 1, 2, 3$) processes.

Since it is difficult to assign the $Y(10750)$ and $\Upsilon(10860)$ as the pure S - and D -wave $b\bar{b}$ states simultaneously, we consider the possibilities of $Y(10750)$ and $\Upsilon(10860)$ as the $\Upsilon(5S)$ -

$\Upsilon_1(4D)$ mixed states with the following mixing scheme

$$\begin{pmatrix} Y(10750) \\ \Upsilon(10860) \end{pmatrix} = \begin{pmatrix} \cos \theta & \sin \theta \\ -\sin \theta & \cos \theta \end{pmatrix} \begin{pmatrix} \Upsilon_1(4D) \\ \Upsilon(5S) \end{pmatrix}. \quad (13)$$

The decay widths of $Y(10750)$ and $\Upsilon(10860)$ versus the mixing angle θ are presented in Fig. 2. In Refs. [13, 14], Badalian *et al.* studied the dielectron widths of the vector bottomonium states, their results indicate that there might be sizeable $S - D$ mixing between the nS - and $(n - 1)D$ -wave ($n \geq 4$) vector states with a mixing angle $\sim 27^\circ$. With this mixing angle, the decay widths of $Y(10750)$ and $\Upsilon(10860)$ can be reasonably understood (see Fig. 2).

The $S - D$ mixing mechanics can shift the masses of the pure states $\Upsilon(5S)$ and $\Upsilon_1(4D)$ to the physical states $Y(10750)$ and $\Upsilon(10860)$. The Hamiltonian of the physical states is assumed to be

$$H = H_0 + H_I, \quad (14)$$

where H contributes diagonal elements to the mass matrix, while H_I could contribute non-diagonal elements to the mass matrix causing the $S - D$ mixing. Then, the masses of $Y(10750)$ and $\Upsilon(10860)$ can be determined by

$$M[\Upsilon(10860)] = \langle \Upsilon(10860) | H_0 + H_I | \Upsilon(10860) \rangle, \quad (15)$$

$$M[Y(10750)] = \langle Y(10750) | H_0 + H_I | Y(10750) \rangle. \quad (16)$$

Combining the mixing scheme defined in Eq.(13), one finds that

$$M[\Upsilon(10860)] = M[\Upsilon_1(4D)] \sin^2 \theta + M[\Upsilon(5S)] \cos^2 \theta - \Delta M_{SD} \sin(2\theta), \quad (17)$$

$$M[Y(10750)] = M[\Upsilon_1(4D)] \cos^2 \theta + M[\Upsilon(5S)] \sin^2 \theta + \Delta M_{SD} \sin(2\theta), \quad (18)$$

where $M[\Upsilon(5S)] = \langle \Upsilon(5S) | H | \Upsilon(5S) \rangle$ and $M[\Upsilon_1(4D)] = \langle \Upsilon_1(4D) | H | \Upsilon_1(4D) \rangle$ correspond to the masses of the pure states $\Upsilon(5S)$ and $\Upsilon_1(4D)$, respectively, while $\Delta M_{SD} = \langle \Upsilon_1(4D) | H_I | \Upsilon(5S) \rangle$ corresponds to the non-diagonal element. Taking a sizeable mixing angle $\theta \sim 20 - 30^\circ$ and a negative value $\Delta M_{SD} \sim -100$ MeV in Eq.(17), one finds that the physical masses of both $Y(10750)$ and $\Upsilon(10860)$ can be consistent with the experimental observations. Thus, with the $S - D$ mixing one may overcome the puzzle that the observed mass of $\Upsilon(10860)$ is obviously higher than the predicted masses of pure $\Upsilon(5S)$ in the potential models.

As a pure $\Upsilon(5S)$ state, the dielectron width of $\Upsilon(10860)$ is predicted to be $\Gamma_{ee} = 0.348$ keV in a recent work [11]. Combining it with the mixing angle $\theta \simeq 27^\circ$ suggested in Ref. [13, 14] we obtain dielectron width $\Gamma_{ee} = 0.28$ keV for $\Upsilon(10860)$, which is consistent with the measured value 0.31 ± 0.07 keV [45]. As a mixed state containing sizeable S -wave component the dielectron width of $Y(10750)$ is estimated to be ~ 0.07 keV. Neglecting the effect of phase space, one may predict the ratio between the production rates of $Y(10750)$ and $\Upsilon(10860)$ in the $e^+e^- \rightarrow \Upsilon(nS)\pi^+\pi^-$ ($n = 1, 2, 3$) processes, i.e.,

$$R \sim \frac{\Gamma_{ee}[Y(10750)]}{\Gamma_{ee}[\Upsilon(10860)]} \simeq \frac{1}{4}, \quad (19)$$

which can explain the observations that production cross sections of $Y(10750)$ are comparable with those of $\Upsilon(10860)$ in the $e^+e^- \rightarrow \Upsilon(nS)\pi^+\pi^-$ ($n = 1, 2, 3$) processes.

From Fig. 2, one can see that the partial widths of the strong decay modes and the ratios between them for the $Y(10750)$ and $\Upsilon(10860)$ resonances are sensitive to the mixing angle. If taking the mixing angle as $\theta \sim 30^\circ$, the decays of $\Upsilon(10860)$ are dominated by the B^*B^* , BB and $B_s^*B_s^*$ channels, while the decays of $Y(10750)$ might be governed by both the B^*B^* and BB^* channels. The large decay rates of $\Upsilon(10860)$ into the $B_s^*B_s^*$ channel can explain the observations at Belle [46] that the $B_s^*B_s^*$ cross section shows a prominent $\Upsilon(10860)$ signal, while the $B_s^*B_s$ and B_sB_s cross sections are relatively small and do not show any significant structures. From the Review of Particle Physics [45], the branching ratios of BB , BB^* , B^*B^* , B_sB_s , $B_sB_s^*$, and $B_s^*B_s^*$ decay modes are $5.5 \pm 1.0\%$, $13.7 \pm 1.6\%$, $38.1 \pm 3.4\%$, $0.5 \pm 0.5\%$, $1.35 \pm 0.32\%$, and $17.6 \pm 2.7\%$, respectively. From Table IV, it can be seen that these branching ratios of $\Upsilon(10860)$ can be hardly described in the pure $\Upsilon(5S)$ interpretation, which is consistent with the analysis in Refs. [8, 9, 11]. With the mixing scheme, this problem can be partially overcome. Our results show that the B^*B^* dominates in the non-strange final channels and the $B_s^*B_s^*$ is prominent in the strange decay modes, which is consistent with the experimental data. However, the predicted large BB partial decay width is still in conflicting with the observations. More theoretical and experimental investigations are needed to clarify this puzzle.

The intermediate B^*B^* meson loop may play an important role in the $S - D$ mixing between $\Upsilon(5S)$ and $\Upsilon_1(4D)$. From Table II, it is seen that both $\Upsilon(5S)$ and $\Upsilon_1(4D)$ states strongly couple to the B^*B^* channel, thus, intermediate B^*B^* meson loop may contribute a sizeable non-diagonal element to the mass matrix, which leads to the $S - D$ mixing. It is interesting to find that the mixing mechanism of axial-vectors $D_{s1}(2460)$ and $D_{s1}(2536)$ has been studied via intermediate hadron loops, e.g. DK , to which both states have strong couplings in Ref. [47]. Also, the $S - D$ mixing scheme of $\psi(4S)$ and $\psi_1(2D)$ states via the meson loops are investigated in Ref. [48]. Their results indicate that the intermediate hadron loops as the mixing mechanism can lead to strong configuration mixing effects and obvious mass shifts for the physical states.

B. $\Upsilon(10580)$ and $\Upsilon(11020)$

Taking $\Upsilon(10580)$ and $\Upsilon(11020)$ as the $\Upsilon(4S)$ and $\Upsilon(6S)$ states, respectively, their masses can be well described in the potential models (see Table I). Furthermore, their decay widths can be reasonably understood within the uncertainties (see Table II). However, their dielectron widths are overestimated as the pure S -wave states [11, 13]. To explain the dielectron widths, in Ref. [13], Badalian *et al.* suggested a $S - D$ mixing in the physical states $\Upsilon(10580)$ and $\Upsilon(11020)$.

We also consider the $\Upsilon(11020)$ resonance as a mixed state via the $\Upsilon(6S)$ - $\Upsilon_1(5D)$ mixing. The mixing scheme is adopted

as follows:

$$\begin{pmatrix} \Upsilon(M_x) \\ \Upsilon(11020) \end{pmatrix} = \begin{pmatrix} \cos \theta & \sin \theta \\ -\sin \theta & \cos \theta \end{pmatrix} \begin{pmatrix} \Upsilon_1(5D) \\ \Upsilon(6S) \end{pmatrix}. \quad (20)$$

The strong decay width of $\Upsilon(11020)$ versus the mixing angle θ is plotted in Fig. 3. It is seen that the total decay width is consistent with experimental data when the mixing angle varies in large range. The current total decay width alone cannot determine the mixing angle. However, the significant leptonic decay width up to 0.130 ± 0.030 keV, indicates the $\Upsilon(11020)$ has a large S -wave component at least.

From the predicted strong decay properties of $\Upsilon(6S)$ and $\Upsilon_1(5D)$ states listed in Table II, one find that $\Upsilon(6S)$ and $\Upsilon_1(5D)$ states mainly couple to two different channels BB^* and B^*B^* , respectively. Furthermore, both $\Upsilon(6S)$ and $\Upsilon_1(5D)$ states are far from the thresholds of BB^* and B^*B^* . Thus, the $\Upsilon(6S)$ - $\Upsilon_1(5D)$ mixing effect via virtual meson loops may be smaller than that of $\Upsilon(5S)$ - $\Upsilon_1(4D)$. If the intermediate meson loops are the main mechanism causing the $S - D$ mixing, the mixing angle for $\Upsilon(6S)$ - $\Upsilon_1(5D)$ should be smaller than that for $\Upsilon(5S)$ - $\Upsilon_1(4D)$. To sum up, although the $\Upsilon(6S)$ - $\Upsilon_1(5D)$ mixing with a small $5D$ -wave component assignment cannot be excluded, we prefer to assign $\Upsilon(11020)$ as the pure $\Upsilon(6S)$ state. In Ref. [35] the authors also expected that there may be less $S - D$ mixing for the $\Upsilon(6S)$ state with the consideration of coupled-channel effects. To better understand the nature of $\Upsilon(11020)$, the missing $\Upsilon_1(5D)$ is worth looking for in future experiments. Our predictions of the mass and strong decay widths of $\Upsilon_1(5D)$ may provide helpful information for future experimental observations.

Besides the possibility of $\Upsilon(5S)$ - $\Upsilon_1(4D)$ and $\Upsilon(6S)$ - $\Upsilon_1(5D)$ mixing, taking the same mixing scheme the decay width of $\Upsilon(10580)$ as $\Upsilon(4S)$ - $\Upsilon_1(3D)$ mixing is also shown in Fig. 4. The total decay width varies dramatically with the mixing angle, and the zero mixing angle is more favored (actually, we use this case to determine the quark pair creation strength γ). From Table II, it is found that the $\Upsilon(4S)$ state mainly couples to the BB channel, and $\Upsilon_1(3D)$ state has strong coupling with the BB^* mode, which suggests that the $\Upsilon(4S)$ - $\Upsilon_1(3D)$ mixing effects via virtual meson loops may be negligible. Thus, if the intermediate meson loops are the main mechanism causing the $S - D$ mixing, and the mixing effects can be neglected. It should be mentioned that in Ref. [35] the authors expected that there may sizeable $S - D$ mixing for the $\Upsilon(4S)$ state with the consideration of coupled-channel effects. It should mentioned that the $\Upsilon_1(3D)$ state might be a narrow state with a width of about 20 - 30MeV according to our calculations, its decays are governed by the BB^* mode, this decay mode might be suitable to be observed in experiments. Looking for the missing $\Upsilon_1(3D)$ state is useful for better understanding the nature of $\Upsilon(10580)$.

V. SUMMARY

In this paper, we calculate the spectrum of the higher vector bottomonium states above the $B\bar{B}$ threshold within both

TABLE II: Strong decay properties for the higher vector bottomonium states predicted within both LP and SP models. For a comparison, other results predicted in the recent works [8, 9, 11] are also listed in the same table.

State (LP/SP)	Decay mode	LP		SP		Ref. [11]		Ref. [8]		Ref. [9]		
		$\Gamma_{th}(\text{MeV})$	$B_r(\%)$	$\Gamma_{th}(\text{MeV})$	$B_r(\%)$	$\Gamma_{th}(\text{MeV})$	$B_r(\%)$	$\Gamma_{th}(\text{MeV})$	$B_r(\%)$	$\Gamma_{th}(\text{MeV})$	$B_r(\%)$	
4^3S_1 (10581/10597)	BB	19.58	100	20.25	100	24.7	100	22.0	100	20.59	100	
	Total	19.58	100	20.25	100	24.7	100	22.0	100	20.59	100	
5^3S_1 (10794/10811)	BB	0.96	2.23	2.25	7.26	13.7	30.0	5.35	19.5	6.22	22.29	
	BB^*	1.76	4.09	≈ 0	≈ 0	26.5	58.1	16.6	60.6	11.83	42.41	
	B^*B^*	33.73	78.37	21.77	70.23	2.58	5.66	2.42	8.83	0.09	0.32	
	B_sB_s	≈ 0	≈ 0	0.30	0.97	0.484	1.06	0.157	0.573	0.96	3.45	
	$B_s^*B_s$	6.59	15.31	6.68	21.55	1.49	3.28	0.833	3.04	1.15	4.11	
	$B_s^*B_s^*$					0.872	1.91	2.00	7.30	7.65	27.42	
	Total	43.04	100	31.00	100	45.6	100	27.4	100	27.89	100	
6^3S_1 (10986/10997)	BB	3.22	26.86	3.80	18.90	7.81	20.4	1.32	3.89	4.18	5.28	
	BB^*	5.69	47.46	9.02	44.85	16.5	43.0	7.59	22.4	15.49	19.57	
	B^*B^*	0.44	3.67	3.13	15.56	4.43	11.5	5.89	17.4	11.87	14.99	
	B_sB_s	0.38	3.17	0.28	1.39	0.101	0.263	1.31	0.00386	0.07	0.09	
	$B_s^*B_s$	1.94	16.18	2.38	11.83	0.780	2.04	0.136	0.401	1.50	1.89	
	$B_s^*B_s^*$	0.32	2.67	1.50	7.46	0.448	1.17	0.310	0.914	2.02	2.56	
	$BB(1P)$						8.27	21.6	7.81	23.0	40.08	50.64
	Total	12.4	100	20.11	100	38.3	100	33.9	100	79.16	100	
3^3D_1 (10646/10658)	BB	≈ 0	≈ 0	0.95	3.41	5.47	10.1	23.8	23.0	
	BB^*	26.41	100	18.76	67.39	15.2	28.1	0.245	0.236	
	B^*B^*			8.13	29.20	33.4	61.8	79.5	76.7	
	Total	26.41	100	27.84	100	54.1	100	103.6	100	
4^3D_1 (10846/10858)	BB	11.82	30.17	12.84	23.87	27.4	31.4	3.85	5.36	
	BB^*	5.55	14.17	7.45	13.85	15.1	17.3	14.0	19.5	
	B^*B^*	18.25	46.58	27.28	50.71	42.1	48.3	50.6	70.5	
	B_sB_s	1.67	4.3	1.86	3.48	0.560	0.642	0.101	0.141	
	$B_s^*B_s$	0.05	0.13	0.62	1.15	0.360	0.412	0.332	0.462	
	$B_s^*B_s^*$	1.84	4.70	3.75	6.97	1.66	1.91	2.94	4.09	
	Total	39.18	100	53.8	100	87.2	100	71.8	100	
5^3D_1 (11029/11036)	BB	8.28	14.27	8.13	10.39	20.0	16.4	
	BB^*	7.89	13.60	8.49	10.85	19.3	15.8	
	B^*B^*	24.08	41.51	27.41	35.02	47.1	38.7	
	B_sB_s	≈ 0	≈ 0	0.02	0.03	0.0235	0.0193	
	$B_s^*B_s$	0.44	0.76	0.36	0.46	0.103	0.0844	
	$B_s^*B_s^*$	2.91	5.02	2.60	3.32	0.798	0.656	
	$B^*B(1^3P_0)$	7.92	13.65	10.08	12.88	3.02	2.48	
	$BB(1P)$	6.49	11.19	13.56	17.33	4.08	3.35	
	$BB(1P')$			7.61	9.72	18.1	14.8	
	Total	58.01	100	78.26	100	121.7	100	

TABLE III: Strong decays for the $\Upsilon_1(4D)$ which is assigned to be $Y(10750)$ or $\Upsilon(10860)$ within the screened potential model.

State	Mode	$Y(10750)$		$\Upsilon(10860)$	
		$\Gamma_{th}(\text{MeV})$	$B_r(\%)$	$\Gamma_{th}(\text{MeV})$	$B_r(\%)$
4^3D_1	BB	≈ 0	≈ 0	13.82	16.98
	BB^*	4.46	13.77	11.92	14.65
	B^*B^*	25.53	78.84	43.17	53.04
	B_sB_s	2.39	7.38	0.97	1.19
	$B_s^*B_s$			2.16	2.65
	$B_s^*B_s^*$			9.35	11.49
	Total		32.38	100	81.39

TABLE IV: Strong decays for the $\Upsilon(5S)$ which is assigned to be $Y(10750)$ or $\Upsilon(10860)$ within the screened potential model.

State	Mode	$Y(10750)$		$\Upsilon(10860)$	
		$\Gamma_{th}(\text{MeV})$	$B_r(\%)$	$\Gamma_{th}(\text{MeV})$	$B_r(\%)$
5^3S_1	BB	0.20	0.38	7.46	16.95
	BB^*	15.63	29.50	20.84	47.34
	B^*B^*	35.52	67.03	8.26	18.76
	B_sB_s	1.64	3.09	1.02	2.31
	$B_s^*B_s$			5.63	12.79
	$B_s^*B_s^*$			0.81	1.84
	Total		52.99	100	44.02

screened and linear potential models. Then, using the pre-

dicted masses and wave functions of these higher vector bottomonium states, their two-body OZI-allowed strong decays are investigated in the 3P_0 model.

Combining the productions, mass, and decay width of the higher vector bottomonium states with each other, we conclude that $Y(10750)$ and $\Upsilon(10860)$ might not be pure S -wave and D -wave vector bottomonium states. Then, we further discuss the possibility of $\Upsilon(10860)$ and $Y(10750)$ as mixed states via the $S - D$ mixing. Our results suggest that $Y(10750)$ and $\Upsilon(10860)$ might be mixed states via the $5^3S_1 - 4^3D_1$ mixing with a sizeable mixing angle $\theta \approx 20^\circ - 30^\circ$. The components of $Y(10750)$ and $\Upsilon(10860)$ are dominated by the 4^3D_1 and 5^3S_1 states, respectively.

Moreover, the strong decay behaviors of the $\Upsilon(10580)$ and $\Upsilon(11020)$ resonances are also discussed. If the $\Upsilon(10580)$ and $\Upsilon(11020)$ resonances are assigned as the $\Upsilon(4S)$ and $\Upsilon(6S)$ states, respectively, their observed widths together with masses are consistent with the theoretical predictions.

Finally, it should be mentioned that the mechanism for the $S - D$ mixing is not clear. If $Y(10750)$ and $\Upsilon(10860)$ as mixed states, several questions should be clarified in future works: (i) what causes the mixing between the 5^3S_1 and 4^3D_1 states; (ii) and how the masses of the pure S - and D -wave states are shifted to the physical states by the configuration mixing.

Acknowledgements

This work is supported by the National Natural Science Foundation of China under Grants No. 11775078, No. U1832173, No. 11705056, and No. 11405053.

-
- [1] A. Abdesselam *et al.* [Belle Collaboration], Observation of a new structure near 10.75 GeV in the energy dependence of the $e^+e^- \rightarrow \Upsilon(nS)\pi^+\pi^-$ ($n = 1, 2, 3$) cross sections, arXiv:1905.05521.
- [2] Z. G. Wang, Vector hidden-bottom tetraquark candidate: $Y(10750)$, arXiv:1905.06610.
- [3] B. Q. Li and K. T. Chao, Bottomonium Spectrum with Screened Potential, *Commun. Theor. Phys.* **52**, 653 (2009).
- [4] C. Meng and K. T. Chao, Scalar resonance contributions to the dipion transition rates of Upsilon(4S,5S) in the re-scattering model, *Phys. Rev. D* **77**, 074003 (2008).
- [5] E. Eichten, S. Godfrey, H. Mahlke and J. L. Rosner, Quarkonia and their transitions, *Rev. Mod. Phys.* **80**, 1161 (2008).
- [6] D. Ebert, R. N. Faustov and V. O. Galkin, Spectroscopy and Regge trajectories of heavy quarkonia and B_c mesons, *Eur. Phys. J. C* **71**, 1825 (2011).
- [7] J. Ferretti and E. Santopinto, Higher mass bottomonia, *Phys. Rev. D* **90**, 094022 (2014).
- [8] S. Godfrey and K. Moats, Bottomonium Mesons and Strategies for their Observation, *Phys. Rev. D* **92**, 054034 (2015).
- [9] J. Segovia, P. G. Ortega, D. R. Entem and F. Fernández, Bottomonium spectrum revisited, *Phys. Rev. D* **93**, 074027 (2016).
- [10] W. J. Deng, H. Liu, L. C. Gui and X. H. Zhong, Spectrum and electromagnetic transitions of bottomonium, *Phys. Rev. D* **95**, 074002 (2017).
- [11] J. Z. Wang, Z. F. Sun, X. Liu and T. Matsuki, Higher bottomonium zoo, *Eur. Phys. J. C* **78**, 915 (2018).
- [12] T. Wei-Zhao, C. Lu, Y. You-Chang and C. Hong, Bottomonium states versus recent experimental observations in the QCD-inspired potential model, *Chin. Phys. C* **37**, 083101 (2013).
- [13] A. M. Badalian, B. L. G. Bakker and I. V. Danilkin, Dielectron widths of the S-, D-vector bottomonium states, *Phys. Atom. Nucl.* **73**, 138 (2010).
- [14] A. M. Badalian, B. L. G. Bakker and I. V. Danilkin, On the possibility to observe higher n^3D_1 bottomonium states in the e^+e^- processes, *Phys. Rev. D* **79**, 037505 (2009).
- [15] A. Ali, C. Hambrock and M. J. Aslam, A Tetraquark interpretation of the BELLE data on the anomalous $\Upsilon(1S)\pi^+\pi^-$ and $\Upsilon(2S)\pi^+\pi^-$ production near the $\Upsilon(5S)$ resonance, *Phys. Rev. Lett.* **104**, 162001 (2010); Erratum: [*Phys. Rev. Lett.* **107**, 049903 (2011)].
- [16] S. Dubynskiy and M. B. Voloshin, Hadro-Charmonium, *Phys. Lett. B* **666**, 344 (2008).
- [17] E. J. Eichten, K. Lane and C. Quigg, Charmonium levels near threshold and the narrow state $X(3872) \rightarrow \pi^+\pi^- J/\psi$, *Phys. Rev. D* **69**, 094019 (2004).
- [18] E. J. Eichten, K. Lane and C. Quigg, New states above charm threshold, *Phys. Rev. D* **73**, 014014 (2006) Erratum: [*Phys. Rev. D* **73**, 079903 (2006)].
- [19] J. L. Rosner, Ψ'' decays to charmless final states, *Annals Phys.* **319**, 1 (2005).
- [20] F. E. Close, C. E. Thomas, O. Lakhina and E. S. Swanson,

- Canonical interpretation of the $D_{sJ}(2860)$ and $D_{sJ}(2690)$, Phys. Lett. B **647**, 159 (2007).
- [21] X. H. Zhong and Q. Zhao, Strong decays of newly observed D_{sJ} states in a constituent quark model with effective Lagrangians, Phys. Rev. D **81**, 014031 (2010).
- [22] X. H. Zhong, Strong decays of the newly observed $D(2550)$, $D(2600)$, $D(2750)$, and $D(2760)$, Phys. Rev. D **82**, 114014 (2010).
- [23] D. M. Li, P. F. Ji, and B. Ma, The newly observed open-charm states in quark model, Eur. Phys. J. C **71**, 1582 (2011).
- [24] D. M. Li and B. Ma, Implication of BaBar's new data on the $D_{s1}(2710)$ and $D_{sJ}(2860)$, Phys. Rev. D **81**, 014021 (2010).
- [25] B. Chen, L. Yuan and A. Zhang, Possible 2S and 1D charmed and charmed-strange mesons, Phys. Rev. D **83**, 114025 (2011).
- [26] H. X. Chen, W. Chen, X. Liu, Y. R. Liu and S. L. Zhu, A review of the open charm and open bottom systems, Rept. Prog. Phys. **80**, 076201 (2017).
- [27] M. S. Liu, Q. F. Lü, X. H. Zhong and Q. Zhao, Fully-heavy tetraquarks, arXiv:1901.02564.
- [28] E. Eichten, K. Gottfried, T. Kinoshita, J. B. Kogut, K. D. Lane and T. M. Yan, The Spectrum of Charmonium, Phys. Rev. Lett. **34**, 369 (1975) Erratum: [Phys. Rev. Lett. **36**, 1276 (1976)].
- [29] E. Eichten, K. Gottfried, T. Kinoshita, K. D. Lane and T. M. Yan, Charmonium: The Model, Phys. Rev. D **17**, 3090 (1978) Erratum: [Phys. Rev. D **21**, 313 (1980)].
- [30] S. Godfrey and N. Isgur, Mesons in a Relativized Quark Model with Chromodynamics, Phys. Rev. D **32**, 189 (1985).
- [31] T. Barnes, S. Godfrey and E. S. Swanson, Higher charmonia, Phys. Rev. D **72**, 054026 (2005).
- [32] B. Q. Li and K. T. Chao, Higher Charmonia and X,Y,Z states with Screened Potential, Phys. Rev. D **79**, 094004 (2009).
- [33] Y. B. Ding, K. T. Chao and D. H. Qin, Screened $Q\bar{Q}$ potential and spectrum of heavy quarkonium, Chin. Phys. Lett. **10**, 460 (1993).
- [34] J. F. Liu and G. J. Ding, Bottomonium Spectrum with Coupled-Channel Effects, Eur. Phys. J. C **72**, 1981 (2012).
- [35] Y. Lu, M. N. Anwar and B. S. Zou, Coupled-Channel Effects for the Bottomonium with Realistic Wave Functions, Phys. Rev. D **94**, 034021 (2016).
- [36] Chong-Hai Cai and Lei Li, Radial equation of bound state and binding energies of Ξ^- hypernuclei, Chin. Phys. C **27**, 1005 (2003).
- [37] W. J. Deng, H. Liu, L. C. Gui and X. H. Zhong, Charmonium spectrum and their electromagnetic transitions with higher multipole contributions, Phys. Rev. D **95**, 034026 (2017).
- [38] L. Micu, Decay rates of meson resonances in a quark model, Nucl. Phys. B **10**, 521 (1969).
- [39] A. Le Yaouanc, L. Oliver, O. Pene, and J. C. Raynal, Naive quark pair creation model of strong interaction vertices, Phys. Rev. D **8**, 2223 (1973).
- [40] A. Le Yaouanc, L. Oliver, O. Pene, and J.-C. Raynal, Naive quark pair creation model and baryon decays, Phys. Rev. D **9**, 1415 (1974).
- [41] M. Jacob and G. C. Wick, On the general theory of collisions for particles with spin, Ann. Phys. (N.Y.) **7**, 404 (1959) ; **281**, 774 (2000).
- [42] L. C. Gui, L. S. Lu, Q. F. Lü, X. H. Zhong and Q. Zhao, Strong decays of higher charmonium states into open-charm meson pairs, Phys. Rev. D **98**, 016010 (2018).
- [43] Q. Li, M. S. Liu, L. S. Lu, Q. F. Lü, L. C. Gui and X. H. Zhong, Excited bottom-charmed mesons in a nonrelativistic quark model, Phys. Rev. D **99**, 096020 (2019).
- [44] Q. F. Lü, T. T. Pan, Y. Y. Wang, E. Wang, and D. M. Li, Excited bottom and bottom-strange mesons in the quark model, Phys. Rev. D **94**, 074012 (2016).
- [45] M. Tanabashi *et al.* [Particle Data Group], Review of Particle Physics, Phys. Rev. D **98**, 030001 (2018).
- [46] A. Abdesselam *et al.*, Study of Two-Body $e^+e^- \rightarrow B_s^{(*)}\bar{B}_s^{(*)}$ Production in the Energy Range from 10.77 to 11.02 GeV, arXiv:1609.08749 [hep-ex].
- [47] X. G. Wu and Q. Zhao, The mixing of $D_{s1}(2460)$ and $D_{s1}(2536)$, Phys. Rev. D **85**, 034040 (2012).
- [48] Z. Cao and Q. Zhao, Impact of S -wave thresholds $D_{s1}\bar{D}_s + c.c.$ and $D_{s0}\bar{D}_s^* + c.c.$ on vector charmonium spectrum, Phys. Rev. D **99**, 014016 (2019).